Electronic Supplementary Information

for

Bromide-Bridged Palladium(III) Chain Complex Showing Charge Bistability Near Room Temperature

Shohei Kumagai,[a] Shinya Takaishi,*[a] Brian K. Breedlove,[a] Hiroshi Okamoto,[b] Hisaaki Tanaka,[c] Shin-ichi Kuroda,[c] and Masahiro Yamashita*[ad]

[a]Department of Chemistry, Graduate School of Science, Tohoku University, 6-3 Aza-Aoba, Aramaki, Aoba-ku, Sendai 980-8578, Japan.
[b]Department of Advanced Material Science, Graduate School of Frontier Sciences, The University of Tokyo, Kashiwa 277-8561, Japan.
[c]Department of Applied Physics, Graduate School of Engineering, Nagoya University, Furocho, Chikusa-ku, Nagoya 464-8603, Japan.
[d]CREST, JST, 4-1-8 Honcho, Kawaguchi, Saitama 332-0012, Japan.

Contents

Experimental details

Single crystal structure was determined on a Bruker APEX II CCD diffractometer with graphitemonochromed Mo Kα radiation ($\lambda = 0.7107$ Å). X-ray oscillation photographs were taken on a Rigaku Saturn 724 CCD diffractometer with graphite monochromated MoKα radiation ($\lambda = 0.7107$ Å). ESR spectra were measured on a Bruker EMX spectrometer equipped with a gas-flow type cryostat Oxford ESR 900. The absolute value of the spin susceptibility was evaluated by comparing the first integrated ESR spectrum of the external standard, $CuSO_4 \cdot 5H_2O$. Electrical resistivity measurements were carried out using a Keithley 2601 sourcemeter with a constant voltage of 1.0 V-nanovoltmeter. Two-probe method was employed for the measurement, on which gold wire was attached to the crystal by carbon paste. Polarized Raman spectra were measured on a Renishaw Raman spectrometer. Polarized Fourier transform infrared (FT-IR) spectra were measured on JASCO FT/IR-6200YMS combined with JASCO infrared microscope ITR-5000 in transmission mode. Polarized reflectivity spectra were obtained by using a specially designed spectrometer with a 25 cm grating monochromator and an optical microscope. All of the measurements above were carried out by using single crystal of **Mal-C7**. ^{1}H nuclear magnetic resonance (NMR) spectra were measured on a Bruker Avance 500 500 MHz Nuclear Magnetic Resonance Spectrometer. High-resolution electrospray ionization time-of-flight mass (ESI-TOF-MS) spectra were acquired on Waters Xevo G2 Tof. UV-Vis-NIR spectra were measured on Shimadzu UV-3100 in transmission mode. Thin film was fabricated by using Mikasa 1H-D7 spincoater.

All reagents were purchased from Wako, TCI, Aldrich and Mitsuwa Chemical Co. Ltd. (Japan) and used without further purification.

Synthesis of sodium salt of diheptyl sulfomalonate Na(MalC$_7$–Y)

O   O   2ROH, $^{conc.}$H$_2$SO$_4$ O   O   1. HSO$_3$Cl / CH$_2$Cl$_2$, 0 °C   O   O

HO   OH   ─────────────→   RO   OR   ───────────────────────→   RO   OR

                    toluene, Δ   2. NaHCO$_3$ / H$_2$O-EtOH   SO$_3$Na

                    (-R = -C$_7$H$_{15}$)

                                              76%   90%
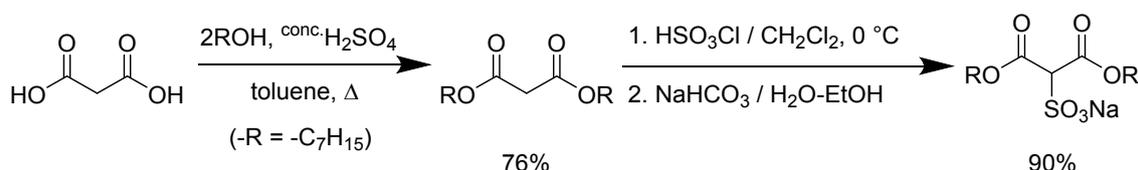
Na(MalC$_7$–Y) was synthesized by slight modification of the previous report.[1] Diheptyl malonate was synthesized from malonic acid and 1-heptanol by the Fischer esterification method with the yield of 76%. Then, obtained diester (6.65 g, 22.1 mmol) was dissolved into dehydrated dichloromethane (20 ml) under N$_2$ atmosphere. The resulting solution was cooled in ice bath, then added 1.48 ml (2.59 g, 22.2 mmol) of chlorosulfonic acid with stirring. After stirred in ice bath for 30 min, pale yellow solution was refluxed for 2 h under N$_2$. Removal of solvent under reduced pressure yielded pale yellow oily liquid. It was dissolved into 50 ml of the mixture of ethanol and water (1/4 (v/v)), added 1.93 g (23.0 mmol) of sodium bicarbonate, and then stirred for 30 min. Resulting solution (pH ≈ 7) was evaporated and dry *in vacuo*, yielding pale yellow solid (7.97 g, 19.8 mmol, 90% based on diheptyl malonate): ^{1}H NMR (500 MHz, DMSO-d_6) δ 0.86 (t, J = 6.9 Hz, 6H), 1.18–1.35 (m, 16H), 1.54 (m, J = 6.9 Hz, 4H), 4.02 (t, J = 6.6 Hz, 4H), 4.39 (s, 1H); ESI-MS (positive) m/z calcd for C$_{17}$H$_{31}$O$_7$SNa$_2$ [M+Na]$^+$ 425.1586, found 425.1620, (negative) m/z calcd for C$_{17}$H$_{31}$O$_7$S [M−Na]$^-$ 379.1790, found 379.1796; Anal Calcd for C$_{17}$H$_{31}$O$_7$SNa: C, 50.73; H, 7.76. Found: C, 47.596; H, 7.650.

Synthesis of sodium salt of didodecyl sulfomalonate Na(MalC$_{12}$–Y)

Na(MalC$_{12}$–Y) was synthesized following the synthetic procedure of Na(MalC$_7$–Y) by using 1-dodecanol instead of 1-heptanol. Yields for didodecyl malonate (white solid) and for sodium salt of didodecyl sulfomalonate (white powder) were 94% based on malonic acid and 92% based on didodecyl malonate, respectively. Analyses for Na(MalC$_{12}$–Y): ^{1}H NMR (500 MHz, DMSO-d_6) δ 0.85 (t, J = 6.9 Hz, 6H), 1.15–1.40 (m, 38H), 1.53 (m, J = 6.9 Hz, 4H), 4.005 (t, J = 6.5 Hz, 2H), 4.008 (t, J = 6.5 Hz, 2H), 4.35 (s, 1H); ESI-MS (positive) m/z calcd for C$_{27}$H$_{51}$O$_7$SNa$_2$ [M+Na]$^+$ 565.3151, found 565.3152, (negative) m/z calcd for C$_{27}$H$_{51}$O$_7$S [M−Na]$^-$ 519.3346, found 519.3356; Anal Calcd for C$_{27}$H$_{51}$O$_7$SNa: C, 59.75; H, 9.47. Found: C, 54.852; H, 9.478.

Crystal growth of Mal-C7

$[Pd(en)_2]Br_2$ (6 mg, 15 μmol) and $Na(MalC_7–Y)$ (12 mg, 30 μmol) were dissolved into methanol/water mixture (3/1 (*v/v*)). Slow diffusion of Br_2 vapor into the solution yielded thin plate-like black crystal of **Mal-C12** within a day: Anal. Calcd for $C_{38}H_{80}BrN_4O_{15}PdS_2$: C, 42.12; H, 7.44; N, 5.17. Found: C, 42.019; H, 7.348; N, 5.208.

Synthesis of Mal-C12

$[Pd(en)_2]Br_2$ (60 mg, 0.16 mmol) and $Na(MalC_{12}–Y)$ (160 mg, 0.30 mmol) were suspended into 10 ml of tetrahydrofuran/water mixture (4/1 (*v/v*)). A drop of Br_2 was dropped into the white suspension, yielding black precipitate. The precipitate was collected by suction filter, then washed with large amount of distilled water. After dried *in vacuo*, 174 mg of black powder was obtained (87% yield based on $Na(MalC_{12}–Y)$): Anal. Calcd for $C_{58}H_{120}BrN_4O_{15}PdS_2$: C, 51.07; H, 8.87; N, 4.11. Found: C, 51.129; H, 8.765; N, 4.047.

Preparation of TF-C12

3 mg of **Mal-C12** was suspended in 1 ml of chloroform. After an ultrasonic treatment for 5 min, the black suspension was heated up until homogeneous pale yellow solution. The solution was immediately cooled by liq. N_2 to be solidified, naturally warmed up to room temperature. The resulting black-green suspension was treated ultrasonication again, then filtered through syringe filter with pore diameter of 1.0 μm. The filtrate was added 30 mg of PMMA, then sonicated for 5 min and left at rest at room temperature for 3 h. The resulting solution was casted onto SiO_2 substrate rotating at 5000 rpm, affording TF-C12.

Table S1. Crystal data and structural refinement parameters for **Mal-C7**.

Radiation type, Wavelength / Å	Mo Kα, 0.71073
Formula	$C_{38}H_{80}BrN_4O_{15}PdS_2$
Formula mass	1083.49
Space group	$P1$
Crystal system	Triclinic
CCDC No.	989698
Crystal size / mm^3	$0.60 \times 0.15 \times 0.02$
a / Å	5.207(3)
b / Å	8.066(5)
c / Å	30.666(19)
α / °	84.437(5)
β / °	89.103(5)
γ / °	86.149(5)
V / Å^3	1278.8(14)
Z	1
T	293(2)
μ / mm^{-1}	1.288
ρ_{calcd} / g cm^{-3}	1.407
$F(000)$	569
GOF on F^2	0.999
R_1, wR_2 [I>2σ(I)]	0.0498, 0.1233
R_1, wR_2 [all data]	0.0560, 0.1269
Reflns. measured	6238
θ Range for data collection / °	4.13–25.38
R_{int}	0.0318
Flack parameter	0.00

Table S2. Selected bond lengths (Å) and angles (°) for **Mal-C7**.

Selected atoms	Value
Pd(1)–Br(1) (Å)	2.6001(18)
	2.6065(18)
Pd(1)–N(1) (Å)	2.032(2)
Pd(1)–N(2) (Å)	2.051(2)
Pd(1)–N(3) (Å)	2.026(3)
Pd(1)–N(4) (Å)	2.033(3)
Br(1)–Pd(1)–Br(1) (°)	179.49(3)
Br(1)–Pd(1)–N(1) (°)	87.77(6)
	91.84(6)
Br(1)–Pd(1)–N(2) (°)	88.15(6)
	91.56(6)
Br(1)–Pd(1)–N(3) (°)	88.30(8)
	91.99(8)
Br(1)–Pd(1)–N(4) (°)	88.03(8)
	92.35(8)
N(1)–Pd(1)–N(2) (°)	96.29(10)
N(1)–Pd(1)–N(3) (°)	83.61(11)
N(1)–Pd(1)–N(4) (°)	179.37(10)
N(2)–Pd(1)–N(3) (°)	179.83(12)
N(2)–Pd(1)–N(4) (°)	83.09(11)
N(3)–Pd(1)–N(4) (°)	97.00(12)

Figure S1. X-ray oscillation photographs of Mal-C7 at various temperature. Red arrows point to the diffuse scatterings.
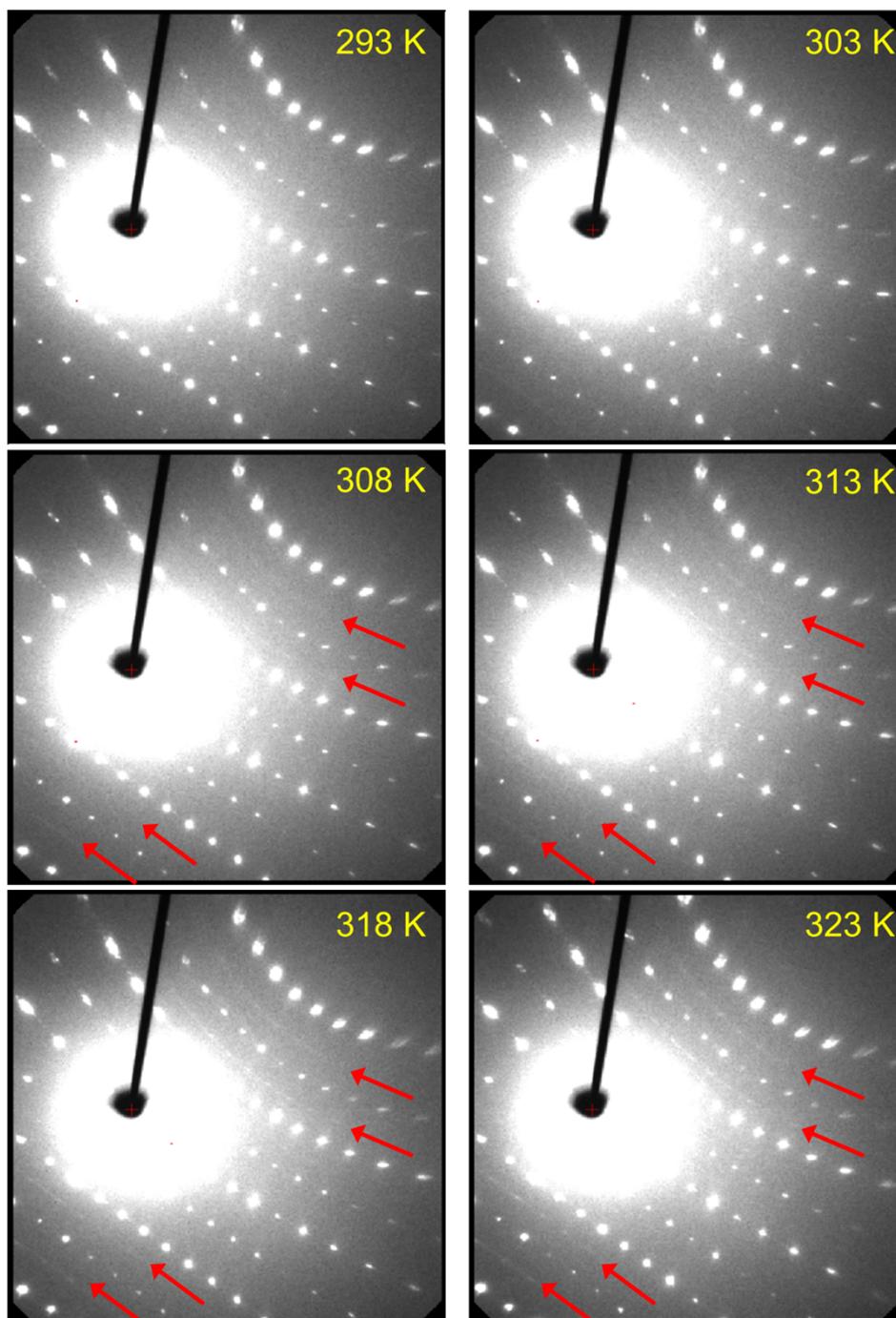
The photographs were taken in the temperature range 293–323 K. X-ray was irradiated for

120 s at each temperature. Upon increasing temperature, weak diffuse scatterings appeared above 308 K. These scatterings indicate a disorder or a distortion of bridging halides, which is characteristic of an MV state. After cooling to 293 K, the X-ray oscillation pattern completely returned to that before raising temperature.

Figure S2. Variable-temperature (VT) ESR spectra for **Mal-C7**.
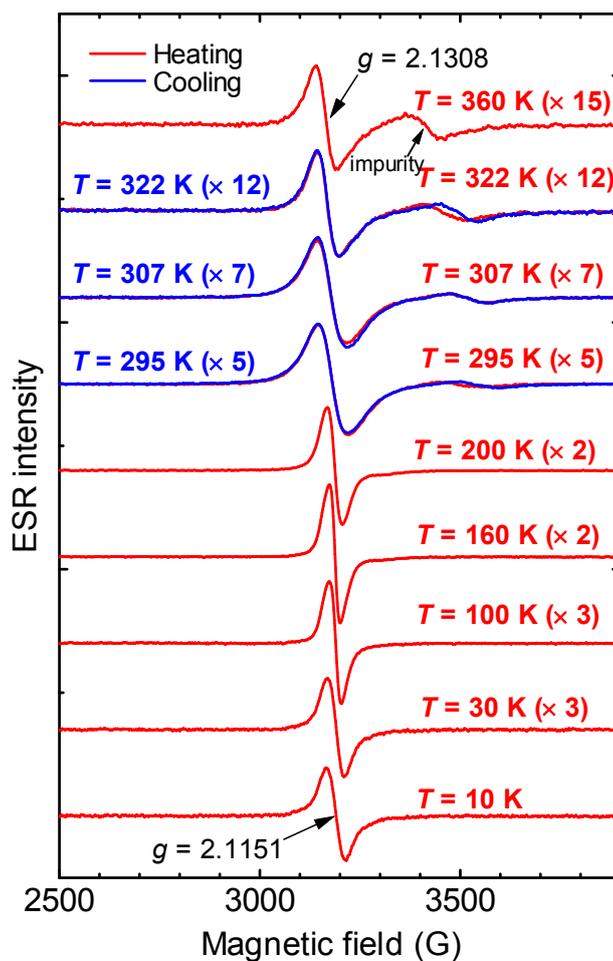
ESR signal for Pd^{III} was observed in the range $2.115 < g < 2.131$ in whole temperature range. The g value got greater and greater upon increasing temperature, indicating the elongation of 1D chain. Another signals which was named impurity were also observed above room temperature. Because, however, those intensities didn't change upon AV–MV conversion, they were ignored on calculation of χ_m.

Figure S3. Temperature dependence of electrical resistivity for **Mal-C7**. Measurement was carried out parallel to 1D chain direction (***a***-axis; $E\|\boldsymbol{a}$). Solid and broken lines reveal heating and cooling processes, respectively. The heating line is the same data as Figure 3b.
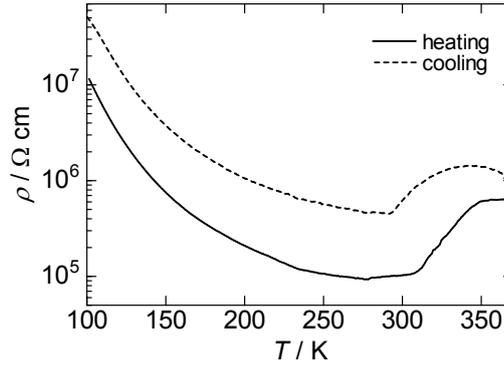
Figure S4. Arrhenius plot for **Mal-C7**. Data were extracted from the heating process. Solid red line is the best fitted line in the range 100–270 K.
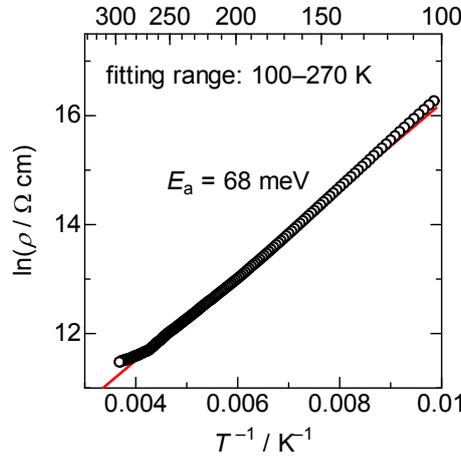
The raw data were fitted by Arrhenius equation:

$$ln(\rho) = ln(\rho_0) + \frac{E_a}{k}\frac{1}{T}$$

where ρ_0, E_a and k represented the electrical resistivity at higher temperature limit, activation energy and Boltzmann constant, respectively. The best fitting in the range 100–270 K (red line in the figure) led us to E_a of 68 meV. This value is much lower than a half of E_{CT} (0.58 eV), although we can assume a relation of $2E_a = E_{CT}$ for an intrinsic semiconductor. This is probably because of the

existence of a small number of Pd^{2+} ions as impurities, i.e., electron carriers, in an as-grown crystal, which is well-known in most of the MX complexes and has been clarified from the measurement of the DC conductivity and the Seebeck coefficient.[2] Therefore, the conventional MX complexes are not intrinsic semiconductors but n-type ones. This nature leads E_a to be lower than a half of E_{CT}.

Figure S5. VT polarized Raman spectra for **Mal-C7**. Polarization is parallel to *a*-axis ($E\|a$).
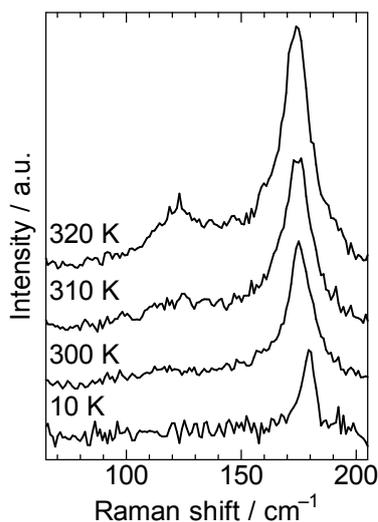
Figure S6. VT polarized IR spectra for **Mal-C7** (left) and the N–H vibrational energy plotted against temperature (right). Polarization is parallel to *b*-axis ($E\|b\perp a$). The data in right figure were extracted from the region meshed by blue shadow in left figure.
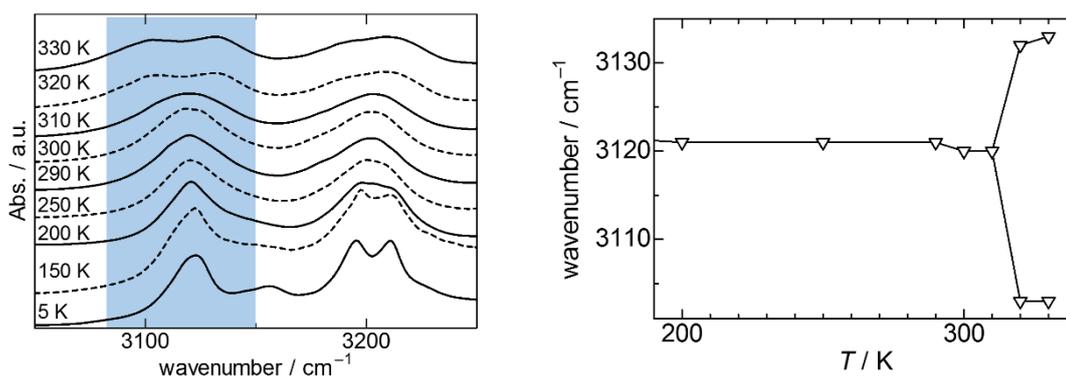
IR signs in the energy region higher than 3150 cm^{-1} may be of O–H stretching modes, so that they are neglected.

Figure S7. VT polarized reflectivity spectra for **Mal-C7**. Polarization is parallel to *a*-axis ($E\|a$).
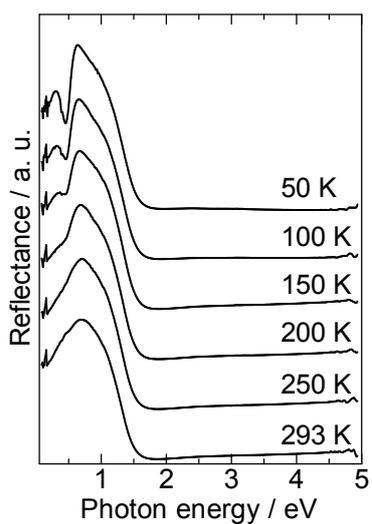
Responses near 0.4 eV are assigned to the backside reflections which are sometimes observed in reflectivity spectra for thin films.

Figure S8. VT optical conductivity spectra for **Mal-C7** ($E\|a$).
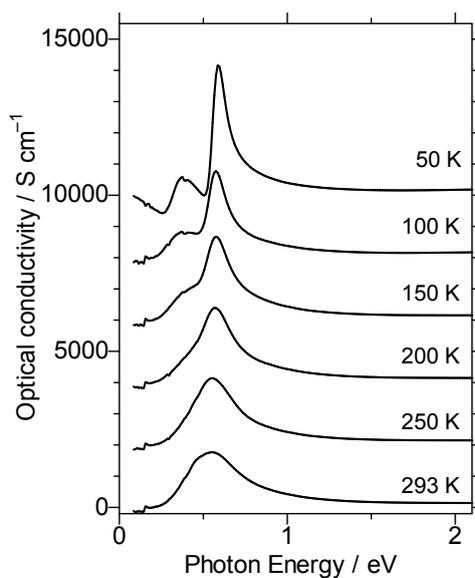
Optical conductivity spectra were obtained by Kramers–Kronig transformation[3] of

polarized reflectivity spectra shown in Figure S7. At each temperature, strong peaks were observed near 0.6 eV accompanied by other responses at lower energy regions. Because the former and the latter are assigned to CT transition and backside reflection, respectively, as mentioned in the footnote to Fig. S7, the latter signals were ignored upon further analyses.

Figure S9. Photographs of thin films of (a) TF-C12 and (b) PMMA.
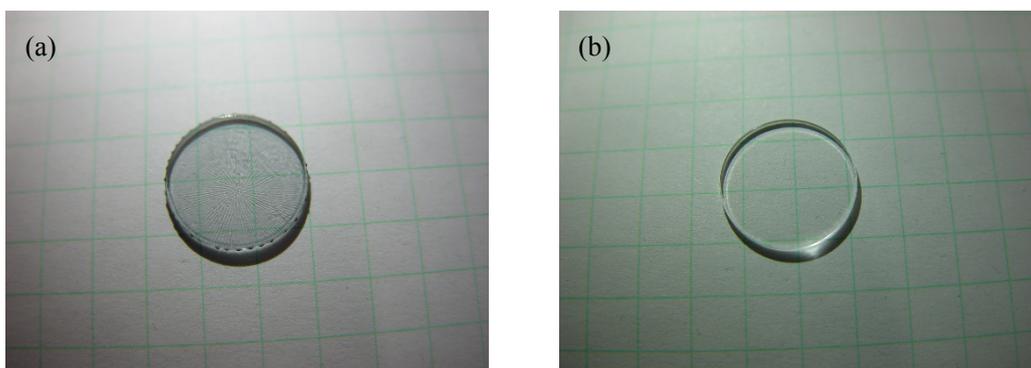
References in Supporting Information
S1   K. G. Naik, C. H. Shar, *J. Indian Chem. Soc.,* 1930, **7**, 111.
S2   S. Iwai, M. Ono, A. Maeda, H. Matsuzaki, H. Kishida, H. Okamoto, Y. Tokura, *Phys. Rev. Lett.*, 2003, 91, 057401 and references therein.
S3   D. M. Roessler, *Brit. J. Appl. Phys.*, 1965, 16, 1119.